

# COSY-11 : How will we remember it ?

Colin Wilkin<sup>1</sup>

*Physics and Astronomy Department, University College London, London, WC1E 6BT, UK*

**Abstract.** A personal selection is made of the highlights of the COSY-11 physics program undertaken at the COoler SYnchrotron of the Forschungszentrum Jülich. This has been particularly rich in the field of strange and non-strange meson production in proton-proton and proton-deuteron collisions. The results are considered in relation to experiments carried out at other facilities and with respect to their impact on theory.

**Keywords:** Meson production, spectrometers and storage rings

**PACS:** 13.75.-n, 13.60.Le, 29.20.-c, 29.30.-h

## INTRODUCTION

Isaac Newton wrote in a famous letter to Robert Hooke: *If I have seen further, it is by standing upon the shoulders of giants*. One of these *giants* was, of course, Nicolaus Copernicus and it is an honor to give this talk in this, his Alma Mater. Innovations in Physics cannot be seen in isolation — they rely heavily on previous work, both theoretical and experimental. Interested people have gone before and (hopefully) will come after.

I have been asked, as an informed outsider, to try to answer the question of how the COSY-11 program fitted into the development of one specialized branch of Physics?

## THE COSY-11 FACILITY

COSY-11 is a very *simple* but effective facility, designed to measure the production of meson(s) in nucleon-nucleon collisions near threshold. *i.e.* at an energy a little above the minimum necessary for the process to happen. It uses the specific characteristics of the COSY = COoler SYnchrotron at the Forschungszentrum Jülich. COSY can accelerate protons up to nearly 3 GeV and store them at a fixed energy (coasting beam) for tens of minutes. This is achieved by having the particles confined in a 180 m vacuum ring by a series of magnets. The magnetic force is just sufficient to counteract the natural tendency for the protons to go in a straight line.

The COSY-11 *trick* relies on the fact that, if the proton loses energy through an interaction in the target, the magnetic force is too strong and the particle is bent to the inside of the ring by an amount that depends upon its momentum. It (or another particle) is then detected by drift chambers, silicon pad detectors, and/or scintillation counters.

---

<sup>1</sup> Email: cw@hep.ucl.ac.uk

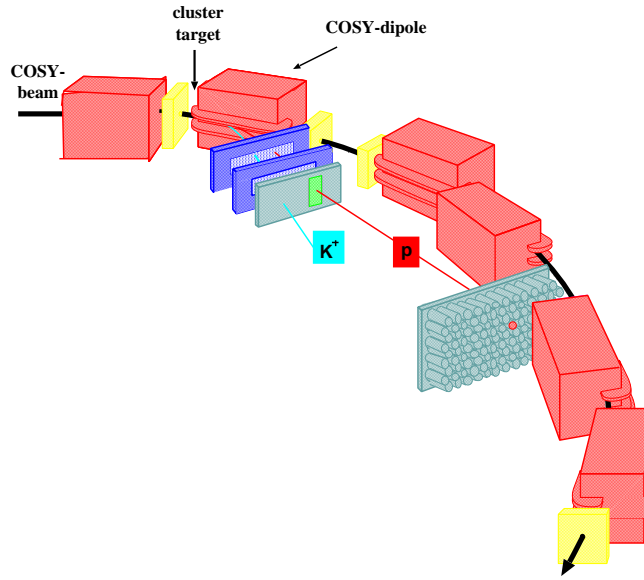


**FIGURE 1.** Schematic diagram of the COSY-11 layout, as illustrated in the COSY-11 calendar for January 1998.

The basic layout and the principal components are shown in the schematic diagram of Fig. 1, but more detailed descriptions are to be found elsewhere in these proceedings.

Most of our body mass is composed of protons and the proton–proton ( $pp$ ) interaction is fundamental. However, above a certain energy mesons can be produced in  $pp$  collisions and so the  $pp$  force cannot be studied in isolation — it is part of a coupled system of nucleons and mesons. For this reason alone it is clear that one must measure production reactions. Because of the uncertainty principle, if mesons with masses of several hundreds of  $\text{MeV}/c^2$  are created, the reaction is going to depend upon the proton–proton force at very short distances — perhaps even shorter than the size of the proton itself.

## THE PRODUCTION OF NON-STRANGE MESONS IN PROTON–PROTON COLLISIONS

To understand the methodology of the COSY-11 technique, we first have to discuss the principles behind a missing-mass measurement. Consider the reaction  $pp \rightarrow ppX$ . If the momenta and hence the energies of two outgoing protons  $p_1$  and  $p_2$  are measured, and those of the beam proton  $p_b$  and target  $p_t$  are known, then the momentum  $\mathbf{p}_X$  and energy  $E_X$  of the system  $X$  are also both known. The mass  $m_X$  of the produced meson can then be calculated from  $m_X^2 = E_X^2 - \mathbf{p}_X^2$ . Thus at COSY-11 one never measured the neutral meson  $X$  directly but rather inferred that it had been produced by considering the kinematics of the other particles in the final state.

Let us look first at the case of  $X = \eta'$ . The  $\eta'$  is a heavy brother of the pion, belonging to the same fundamental pseudoscalar nonet. However, its mass is even a bit bigger than that of the proton. In order to compare results for mesons with widely different masses,

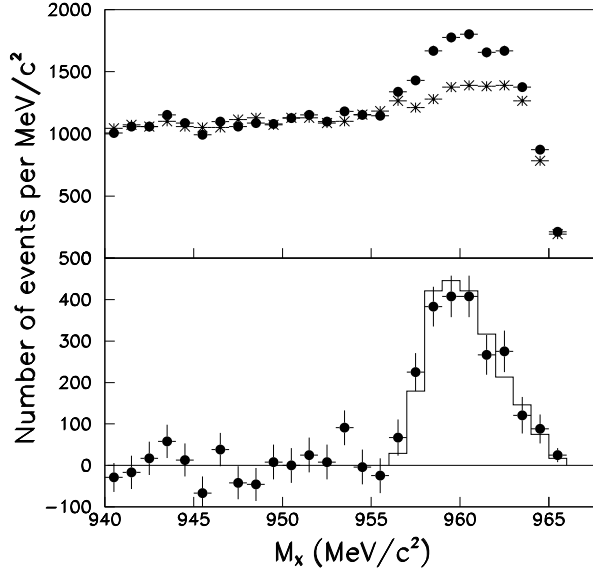


**FIGURE 2.** Missing-mass spectrum of the  $pp \rightarrow ppX$  reaction measured with the SPESIII spectrometer at Saturne at a proton beam energy of  $T_p = 2430 \text{ MeV}$  [1]. In the upper panel the closed circles represent the actual data whereas the crosses are estimates of the background obtained from measurements taken below the reaction threshold. The differences are shown by the points in the lower panel. These are compared to the Monte Carlo simulation of the  $pp \rightarrow pp\eta'$  reaction for  $Q = 8.3 \text{ MeV}$ , which is shown by the histogram.

we normally present data in terms of the kinetic energy in the exit channel. Thus we define the excess energy of the reaction as being  $Q = W - 2m_p - m_X$ , where  $W$  is the total center-of-mass (c.m.) energy.

The basic problems of a missing-mass experiment are the minimization and evaluation of the background under the peak of the  $\eta'$  or other meson. The amount of background is usually decided by doing measurements also below threshold. However, the better the mass resolution, the easier it is to control the background. Having subtracted the suitably scaled background from the actual measurements, one ends up with a peak around the meson mass. This is illustrated in the case of the SPESIII measurements from Saturne [1] which are shown in Fig. 2. The next step is to make sure that the peak that has been generated in this way has the right shape and this is done by doing a computer (Monte Carlo) simulation, where one feeds in as much information about the reaction and the experimental apparatus and conditions as possible. For a spectrometer like COSY-11 or SPESIII, there is a limited coverage of the angles, *i.e.* there is a restricted geometrical acceptance. Furthermore, in certain regions the counters may have limitations and this reduces even further the overall acceptance. The Monte Carlo simulations are of tremendous importance in modern particle and nuclear physics because they allow one to correct to some extent for these deficiencies. The Monte Carlo of the  $\eta'$  peak in Fig. 2 fits the data reasonably well and this gives some confidence in the

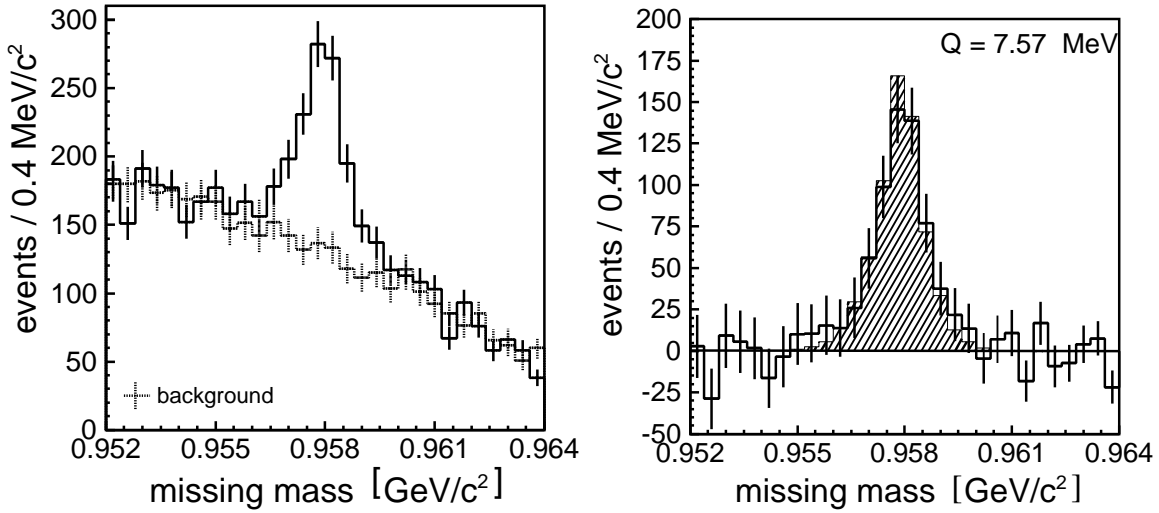


**FIGURE 3.** Missing-mass spectrum from the  $pp \rightarrow ppX$  reaction obtained at an excitation energy of  $Q = 7.57$  MeV with respect to the  $\eta'$  peak [2]. The left panel shows the total count rate in bins of  $0.4 \text{ MeV}/c^2$  (solid histogram) compared to the background that is shown dashed. The difference in the right panel is compared with the Monte Carlo simulation of  $\eta'$  production.

number of  $pp \rightarrow pp\eta'$  events extracted.

The  $pp \rightarrow pp\eta'$  reaction was studied at two energies at SPESIII [1] but it was measured at fifteen energies at COSY-11 [2], the results for one of which is shown in Fig. 3. Both the excitation energy  $Q$  and numbers of  $\eta'$  events were very similar to those of the SPESIII data of Fig. 2. However, the better energy determination at COSY allowed finer mass bins to be used ( $0.4$  rather than  $1.0 \text{ MeV}/c^2$ ). This gives rise to a smoother background but it is important to note that the shape of this background is influenced by the specific characteristics of the spectrometer. This is seen even more clearly for the  $\eta'$  peak itself — the distribution is far more symmetric at COSY-11 and this is what was to be expected on the basis of the Monte Carlo simulation that is also shown in Fig. 3.

One very important parameter is the signal-to-background ratio at the  $\eta'$  peak. This is strongly influenced by the resolution — the narrower the peak the easier it is to isolate its contribution to the production rate. For COSY-11 this is about 1:1 whereas at SPESIII it was only 1:3. It is clear that COSY-11 was very well suited for the study of such production experiments.

The  $pp \rightarrow pp\eta'$  total cross section varies smoothly with excess energy  $Q$  when plotted on the logarithmic scale of Fig. 4. Since the  $\eta'$ -nucleon force is believed to be relatively weak, we would expect that this energy dependence should be largely given by phase space, modified by the effect due to the interaction of the two outgoing protons in the final state. This is particularly strong in the  $S$ -wave because there is a virtual state with a ‘binding’ energy of  $Q_0 \approx 0.45 \text{ MeV}$ .

If only the virtual bound state pole is taken into account, one can easily obtain an analytic expression for the shape of the energy dependence in the non-relativistic

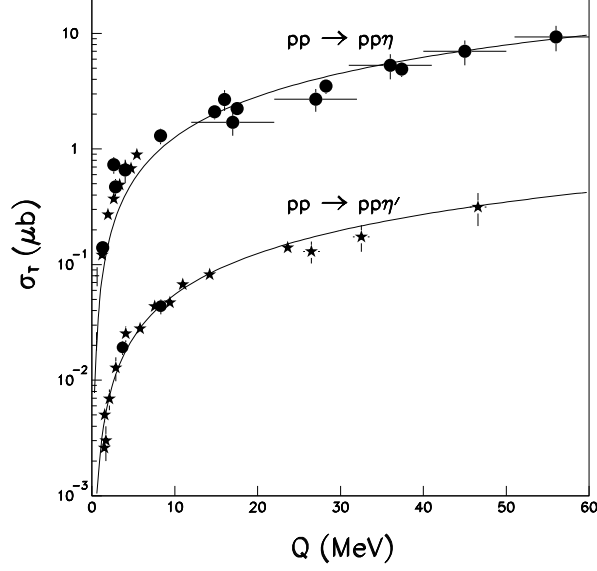


**FIGURE 4.** Variation of the total cross sections for  $pp \rightarrow pp\eta$  and  $pp \rightarrow pp\eta'$  with excess energy  $Q$ . The COSY-11 experimental results, shown by stars, are taken from Refs. [4, 2, 5, 6]. Data of other groups, shown by circles, are from Refs. [1, 7, 8]. The model of Eq. (1), that only includes phase space plus the  $pp$  final state interaction [3], fails to describe the  $\eta$  production data in the near-threshold region, whereas it is perfectly adequate for the  $\eta'$ .

approximation [3]:

$$\sigma_T = \sigma_0 \frac{(Q/Q_0)^2}{\left(1 + \sqrt{1 + Q/Q_0}\right)^2}. \quad (1)$$

Although  $Q_0$  is fixed just by the  $pp$  interaction, the value of  $\sigma_0$  depends on the full dynamics of the  $pp \rightarrow pp\eta'$  reaction. The  $\eta'$  data of Fig. 4, which are completely dominated by measurements from COSY-11, are well represented by this description.

The  $\eta$  meson has a much smaller mass than the  $\eta'$  and several groups have measured the total cross section for  $pp \rightarrow pp\eta$  and a selection of their results is shown in Fig. 4 along with those of  $\eta'$  production. A fascinating point seen here is that, unlike the case of  $\eta'$  production, the *ansatz* of Eq. (1) cannot reproduce simultaneously the low and higher  $Q$  data. The curve underpredicts the data below about 10 MeV. This is almost certainly the signal for a very strong interaction in the final state, where the  $\eta$  bounces between the two protons. For heavier nuclei this final state interaction becomes so strong that the  $\eta$  becomes trapped for some time around the nucleus — but more of this later!

However, one also notices from Fig. 4 that the cross section for  $\eta'$  production is about 25 times smaller than for the  $\eta$ . It is a fairly general feature that, as the mass of the meson is increased, the cross section drops. This is due mainly to the momentum transfer from the initial to the final protons rising with meson mass. On the other hand, the background does not fall in the same way and it becomes increasingly difficult to identify the meson

purely through a missing-mass peak. Coincidence measurements of the photons and pions arising from the decay of the meson are then also required. This is one part of the WASA program which has already started at COSY [9]. For example, the reaction  $pp \rightarrow pp\eta$  has been identified cleanly through the decay chain  $\eta \rightarrow \pi^0\pi^0\pi^0 \rightarrow \gamma\gamma\gamma\gamma\gamma$ . Thus, although COSY-11 has been laid to rest, the succession is assured through the WASA spectrometer [9].

## HYPERON PRODUCTION IN PROTON-PROTON COLLISIONS

The second major COSY-11 success came from measuring  $\Lambda$  and  $\Sigma^0$  production in the  $pp \rightarrow K^+\Lambda p$  and  $pp \rightarrow K^+\Sigma^0 p$  reactions. In such cases one has to study final Kaon-proton correlated pairs instead of the proton-proton required for  $\eta$  and  $\eta'$  production.

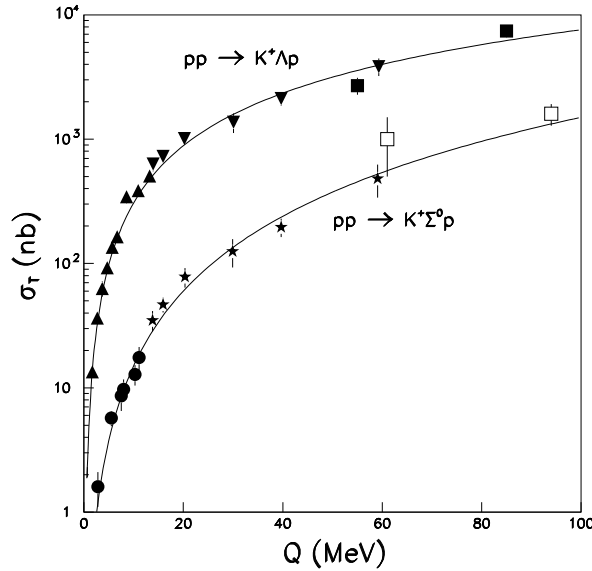


**FIGURE 5.** Total cross sections for hyperon production in  $pp$  collisions as functions of the excess energy  $Q$ . The experimental points for the  $pp \rightarrow K^+\Lambda p$  reaction come from COSY-11 (up and down triangles) [10, 11, 12] and COSY-TOF (closed squares) [13, 14]. The curve corresponds to the predictions of phase space moderated by a final-state interaction between the  $\Lambda$  and the proton. The COSY-11  $pp \rightarrow K^+\Sigma^0 p$  points (closed circles and stars) [11, 12] and two COSY-TOF points (open squares) [13, 15] are compared to phase-space predictions.

$K^+$  are much rarer in the final state than protons and it is not possible to get an unambiguous identification just from the available information on the trajectory and time of flight. Therefore one takes the events around the kaon mass to see if the missing mass then corresponds to a  $\Lambda$  or a  $\Sigma^0$ . In this way islands corresponding to the two reactions can be isolated. Experiments could be done simultaneously at two different energies to compensate for the mass difference of  $m_{\Sigma^0} - m_{\Lambda} = 77 \text{ MeV}/c^2$ . For this purpose the supercycle mode was used, where the beam was accelerated to one energy and left to coast under stable conditions while the  $\Lambda$  production was measured. The beam energy

was then raised further to allow the  $\Sigma^0$  to be studied before the energy was lowered again. The results are shown in Fig. 5.

Apart from a couple of points from COSY-TOF [13, 14], the  $\Lambda$  data are dominated by results from COSY-11 [10, 11, 12]. Although the  $K^+$  interacts weakly with the final proton, the  $\Lambda p$  final-state interaction is known to be quite strong. The  $\Lambda$  does just bind with the deuteron and heavier  $\Lambda$ -hypernuclei have been studied for fifty years. However, though the  $\Lambda p$  force is attractive, it is not quite attractive enough to form a bound state and instead there is a virtual state at an energy of  $Q_0 \approx 5.5$  MeV. If this were the only distortion of phase space, the energy dependence of the cross section would be given by Eq. (1) and the resulting curve does give a good description of the data in the figure with this value of  $Q_0$ .

On the other hand, there is no convincing evidence for the existence of  $\Sigma$ -hypernuclei. While this could be due to their having very large widths engendered by the strong decay  $\Sigma N \rightarrow \Lambda N$ , the COSY-11 data, which dominate Fig. 5, offer a much simpler explanation. The  $pp \rightarrow K^+ \Sigma^0 p$  total cross section follows a phase-space  $Q^2$  variation, *i.e.*,  $Q_0 \rightarrow \infty$  in Eq. (1). This is what we would expect if there were no strong interaction between the  $\Sigma^0$  and the proton. The obvious conclusion is that there are no  $\Sigma$ -hypernuclei because the  $\Sigma$ -nucleon force is not very attractive.

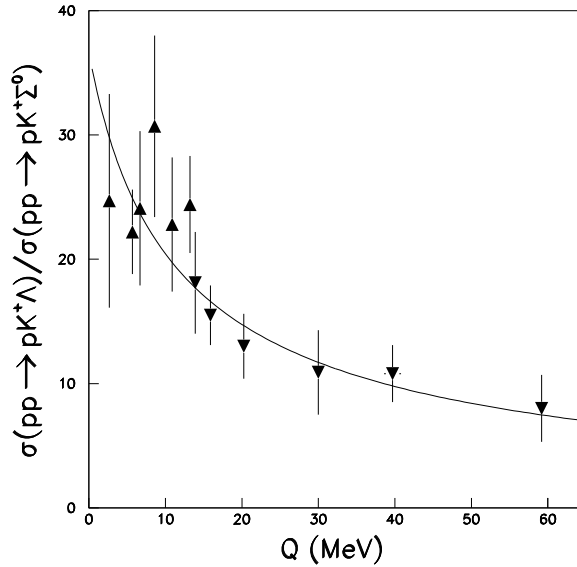


**FIGURE 6.** The ratio of the total cross sections for the  $pp \rightarrow K^+ \Lambda p$  and  $pp \rightarrow K^+ \Sigma^0 p$  reactions at the same values of the excess energy  $Q$ . The COSY-11 points [11, 12] are compared to the predictions of Eq. (2) where a final-state interaction is only invoked in the  $\Lambda p$  channel.

Because of the very different final-state interactions in the  $\Lambda p$  and  $\Sigma^0 p$  systems, the energy dependence of the ratio of their production cross sections is very sharply peaked to  $Q = 0$ , as illustrated in Fig. 6. The data are well described by just including the  $\Lambda p$

interaction, and this leads to:

$$\sigma_T(pp \rightarrow K^+ \Lambda p) / \sigma_T(pp \rightarrow K^+ \Sigma^0 p) = R_0 / \left(1 + \sqrt{1 + Q/Q_0}\right)^2. \quad (2)$$

Here  $Q_0 = 5.5 \text{ MeV}$  is the position of the virtual  $\Lambda p$  state and  $R_0 \approx 147$  depends upon the details of the dynamics of both  $\Lambda$  and  $\Sigma^0$  production.

It is evident that COSY-11 was very well suited for the study of hyperon production in proton–proton reactions. The obvious questions left to be answered are:

- What is the production like in proton–neutron collisions?
- What is the spin dependence of the production with polarized beams and polarized targets?

Experiments at COSY-ANKE and/or COSY-TOF might help to resolve some of these questions — but they will not be easy to carry out! Neutron detection have already been attempted at COSY-11 for the  $pn \rightarrow pn\eta'$  reaction using a deuterium target [16]. For this one has to measure both the low energy *spectator* proton from the deuteron target as well as the fast final neutron. This is clearly an ambitious program given the low overall acceptance but, even with only 19% of the data analyzed, a clear  $\eta'$  signal is seen.

## KAON-PAIR PRODUCTION IN PROTON-PROTON COLLISIONS

Two of the least understood of the light mesons are the scalar (spin-0, positive parity)  $a_0(I=1)/f_0(I=0)$  pair, both of which have masses around  $980 \text{ MeV}/c^2$ . They are found dominantly in the  $\pi\eta$  and  $\pi\pi$  channels, respectively, but are also ‘seen’ in  $K\bar{K}$  [17]. Since the  $K^+K^-$  threshold is at  $987.4 \text{ MeV}/c^2$ , this channel distorts the shapes of the  $a_0/f_0$  resonance peaks — they may even be mainly molecular rather than quark–antiquark states. The question asked at COSY was whether one could measure the production of these resonances in proton–proton collisions through the detection of their  $K^+K^-$  decay branch.

The DISTO collaboration at Saturne measured the cross section for  $pp \rightarrow ppK^+K^-$  at quite high excess energy [18]. However, since the reaction involves a four–body final state, the cross section drops very fast as threshold is approached. On the other hand, the limited angular coverage meant that at COSY-11 the reaction could only be studied near threshold. The protons were measured here as before, using the time of flight from a start to a stop scintillator. Because of its smaller mass the  $K^+$  has a lower momentum near the reaction threshold and is therefore bent more by the analyzing dipole. The start signal for this particle was deduced from the measurement of the two protons rather than being directly determined. One complication is that kaons die quite quickly and this reduced significantly the overall acceptance. Having identified the two protons, as well as a candidate for the  $K^+$ , the final selection of the  $pp \rightarrow ppK^+K^-$  reaction was performed by evaluating the missing mass with respect to the  $ppK^+$  trio and making sure that it was equal to that of the  $K^-$ .

The four lowest energy points in Fig. 7 come from COSY-11 [19, 20, 21], with the higher energy data being measured at ANKE [22] and DISTO [18]. The only distortion



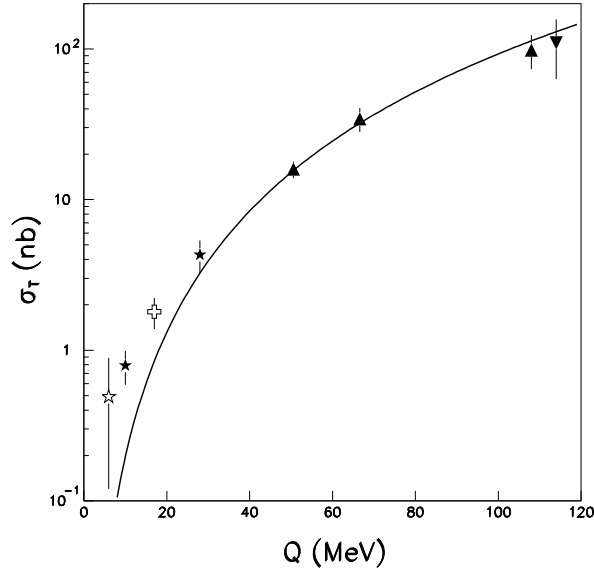


**FIGURE 7.** Total cross section for the  $pp \rightarrow ppK^+K^-$  reaction. The experimental data are taken from Refs. [19] (open star), [20] (open cross), [21] (closed stars), [22] (triangles), and [18] (inverted triangle). For data that were measured above the  $\phi$  threshold, only the contribution from non- $\phi$  production is reported here. The curve is the generalization of Eq. (1) to a four-body phase space, the analytic formula for which is to be found in Ref. [23].

to the four-body phase space considered in the curve is that due to the  $pp$  final-state interaction [23] and, when this is normalized to the high- $Q$  points, it undershoots considerably the data at low  $Q$ . It therefore seems likely that there must be an additional important final-state interaction among the  $ppK^+K^-$  particles. Direct evidence for this is to be found in Fig. 8, where the ratio of the number of events (corrected for acceptance) for  $K^-p$  and  $K^+p$  is plotted against the invariant mass in the  $Kp$  system. There are far more events with low  $K^-p$  invariant mass than  $K^+p$ . Since the  $K^+p$  force is known to be weak, the obvious conclusion to draw is that there is also a strong  $K^-p$  final-state interaction, possibly connected with the influence of the  $\Lambda(1405)$  hyperon resonance that is a little below the  $K^-p$  threshold.

The COSY-11 measurements [21] were made below the threshold for  $\phi$  production and, for the analogous data from ANKE [24, 25], care has to be taken to distinguish between  $\phi$  and non- $\phi$  production. After this has been done, the higher energy data show all the same features as those presented in Fig. 8 but with higher statistics. In fact, the shape of the entire  $N(K^-p)/N(K^+p)$  data set at different energies can be described quantitatively through the introduction of a universal  $K^-p$  final-state interaction [25].

Analogous enhancements of the  $\bar{K}^0d$  invariant-mass spectrum are seen in the  $pp \rightarrow dK^+\bar{K}^0$  reaction [26]. Thus the COSY-11 and the COSY-ANKE data, taken together, quite clearly show that the  $K^-$  is strongly attracted to nucleons and this is likely to develop further for heavier nuclei. On the other hand, the strength of the  $K^-p$  force is

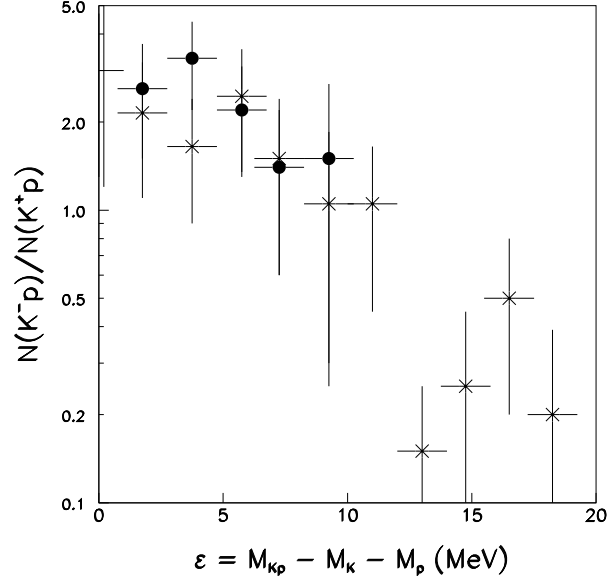


**FIGURE 8.** Ratio of the number of events with the  $K^-p$  and  $K^+p$  in a given invariant mass bin measured from the  $Kp$  threshold. The COSY-11 data at  $Q = 10$  MeV (closed circles) and 28 MeV (crosses) were reported in Ref. [21]. It should be noted that the 10 MeV results have been scaled up by a factor of about 3.5 so that they can be compared more easily with the higher energy results.

such that it will be very hard to extract much information on the  $a_0/f_0$  complex from  $pp \rightarrow ppK^+K^-$  or similar reactions. However, physics is a continuous development. The results in one experiment influence ideas at other facilities and the scalar meson search will be continued at COSY-WASA [9].

## THE $dp \rightarrow {}^3\text{He}\eta$ REACTION

The last example that I have chosen to illustrate the COSY-11 legacy involves  $\eta$  production in the three-nucleon sector. When I discussed the  $pp \rightarrow pp\eta$  reaction I stressed that, unlike the case of the  $\eta'$ , the data seemed to require a strong interaction of the  $\eta$  with one or two of the final protons.

The situation is more extreme for  $dp \rightarrow {}^3\text{He}\eta$  where it has even been speculated that the  $\eta$  might even be trapped, at least momentarily, while going around the  ${}^3\text{He}$  nucleus [27]. Early Saturne measurements of the total cross section near threshold [28, 29] gave strong support for these ideas and the new very refined measurements from COSY-11 [30] and COSY-ANKE [31] show conclusively that there is a pole in the  $dp \rightarrow {}^3\text{He}\eta$  scattering amplitude, corresponding to a quasi-bound or virtual state, within about an MeV of the threshold. The precise number depends upon exactly how one takes the smearing of the beam momentum into account; this can be important when one is discussing the difference between 1.0 or 0.5 MeV!

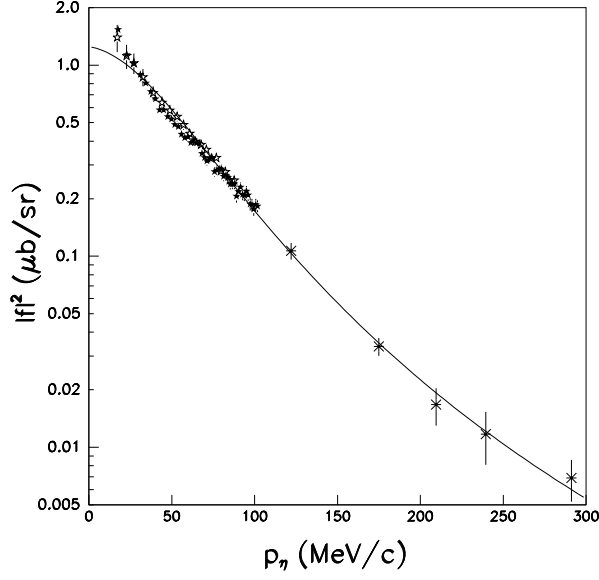


**FIGURE 9.** Square of the backward amplitude for  $dp \rightarrow {}^3\text{He} \eta$ . The refined COSY-11 (open stars) [30] and COSY-ANKE data (closed stars) [31] are hard to distinguish on this plot. The very-close-to-threshold data, which are important in the evaluation of the pole position, are not shown because of the differences in the energy smearing in this region. The early Saturne backwards' measurements are also shown, as is the parameterization taken from the SPESIV paper [28].

The COSY-11 and COSY-ANKE experiments both benefited from the negligible thickness of the target material and the ability of the COSY machine crew to ramp up the energy in fine steps as a function of time. Fortunately, the two data sets are completely consistent within the systematic error bars, as is shown by the plot of the square of the backward production amplitude shown in Fig. 9. This geometry is chosen so that data at higher energy [32] could be shown on the same plot in order to illustrate the continuity of the physics. The curve presented in the figure is the parameterization of the SPESIV low [28] and higher energy data [32]. However, the position of the quasi-bound (or virtual) state pole in the complex  $Q$ -plane depends a lot on the data very close to threshold and this is hard to obtain with an external beam and a macroscopic target [29].

The energy dependence of the  $dp \rightarrow {}^3\text{He} \eta$  total cross section shows that the magnitude of the  $s$ -wave production amplitude  $f_s$  decreases fast with excess energy  $Q$  (or the  $\eta$  center-of-mass momentum  $p_\eta$ ). However, to prove conclusively that  $f_s$  has a pole near  $Q = 0$  it would be highly desirable to show that the phase of  $f_s$  also varies very rapidly in this region. Evidence for this comes from the study of the angular dependence of the cross section [33, 34]. For both the COSY-11 and COSY-ANKE data it is seen that the differential cross section is linear in the cosine of the  $\eta$  angle with respect to the initial proton:

$$\frac{d\sigma}{d\Omega}(dp \rightarrow {}^3\text{He} \eta) \propto 1 + \alpha \cos \theta_{p\eta}. \quad (3)$$

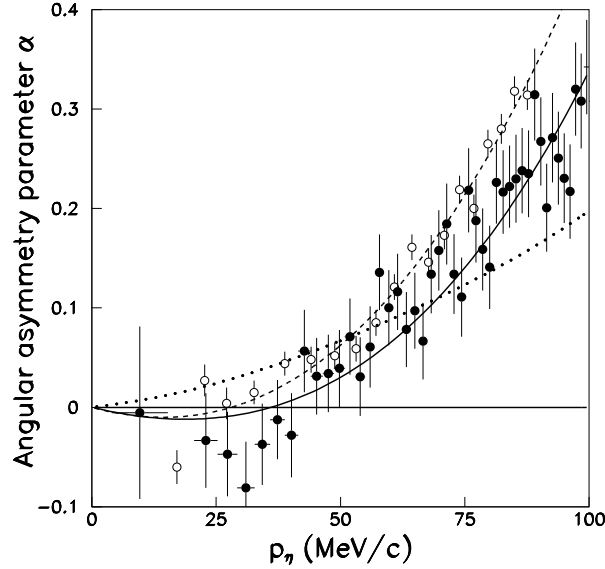


**FIGURE 10.** Angular asymmetry parameter  $\alpha$  of the  $dp \rightarrow {}^3\text{He}\eta$  reaction defined by Eq. (3) as a function of the  $\eta$  c.m. momentum. The experimental data from COSY-ANKE (closed circles) [31] and COSY-11 (open circles) [30] are compared to fits (solid and broken lines) where the phase variation of the  $s$ -wave production amplitude associated with the pole in the complex plane close to  $p_\eta = 0$  is taken into account. If the phase variation is neglected, the best fit (dotted curve) fails to describe the data.

Near threshold, the asymmetry parameter  $\alpha$  must arise from an interference between  $s$ - and  $p$ -waves of the final  ${}^3\text{He}\eta$  system and simple kinematic arguments would suggest that  $\alpha$  should vary linearly with  $p_\eta$  [33]. This is, however, modified a little because of the falling of the magnitude of  $f_s$  with momentum. Nevertheless, if one just takes into account the decrease of  $|f_s|$ , one cannot reproduce the momentum dependence of  $\alpha$  illustrated in Fig. 10. This parameter seems to be small, or possibly even negative, for low  $p_\eta$ , and it is only above about 40–50 MeV/c that it starts to take off. This means that the sign of the  $s$ - $p$  interference must be changing fast with  $p_\eta$  and hence that the phase of  $f_s$  is a very sensitive function of  $p_\eta$ . In Fig. 10 are shown the COSY-11 and COSY-ANKE data with crude fits to the  $\alpha$  variation where the feedback of the  $p$ -waves to the total cross section has been neglected. If, and only if, the phase variation associated with the quasi-bound state pole is included in the fits can the momentum variation of  $\alpha$  be understood. More precise modelling, where the total cross section and angular distributions are fit simultaneously [33, 34], does not change this conclusion in any material way. Both data sets require the magnitude and phase of the  $s$ -wave amplitude to vary in the way expected if there is a pole in  $f_s$  for small  $|Q|$ .

Production data of this kind can never prove whether the pole corresponds to a quasi-bound or a virtual state but, in either case, the COSY data have shown that there is a very unusual nuclear system. This is a tribaryon with an excitation energy of about 550 MeV but a width of only a very few MeV. It is not, of course, stable because it can decay with the emission of nucleons and possibly pions. Hence one of the last of the COSY-11 experiments seems to confirm the existence of this very strange nuclear state.

## FAREWELL COSY-11!

I have lived through the closure of many machines — the Cosmotron at Brookhaven, the CERN SC, the Orsay SC, the Saturne machine at Saclay, and the CELSIUS storage ring at Uppsala. What really matters is the people and how they take what they have learned at one facility and apply it in another environment.

Hadronic physics has advanced because of COSY-11 and there are many possibilities to push even further forward, especially using COSY-WASA [9]. The Polish–German collaboration has been tremendously successful in personal terms; I have found them to be a real delight to work with. The challenge is to ensure that this atmosphere continues in the same way in the larger multinational COSY-WASA setting.

As has been made clear many times in this meeting, the symbol of COSY-11 has been a goat. It is clear that I must have been a supporter of COSY-11 long before the facility was conceived since the ceramic plaque of a goat by Picasso shown in Fig. 11 has been hanging on a dining room wall in my house for the past forty years. The message that I would like to leave you with is that, to a first approximation, goats eat anything — and survive!



**FIGURE 11.** Ceramic plaque of a goat stamped ‘Madoura Plein Feu’ and ‘Empreinte Originale de Picasso’ on the Wilkin wall since 1967.

## ACKNOWLEDGMENTS

I am very grateful to the organizers of the meeting for being offered the opportunity to highlight some of the COSY-11 successes over the years. The selection has been very much a personal one that has been tremendously biased by my own interests and the presentation has been greatly influenced by my own views on the physics involved. Finally, I hope that the goat will enjoy its new pastures.

## REFERENCES

1. F. Hibou *et al.*, Phys. Lett. B **438**, 41–46 (1998).
2. P. Moskal *et al.*, Phys. Lett. B **474**, 416–422 (2000).
3. G. Fäldt and C. Wilkin, Phys. Lett. B **382**, 209–213 (1996).
4. J. Smyrski *et al.*, Phys. Lett. B **474**, 182–187 (2000).
5. P. Moskal *et al.*, Phys. Rev. Lett. **80**, 3202–3205 (1998).
6. A. Khoukaz *et al.*, Eur. Phys. J. A **20**, 345–350 (2004).
7. H. Calén, *et al.*, Phys. Lett. B **366**, 39–43 (1996).
8. H. Calén *et al.*, Phys. Rev. Lett. **79**, 2642–2645 (1997).
9. *WASA at COSY proposal*, Ed. B. Höistad and J. Ritman, arXiv:nucl-ex/0411038.
10. J.T. Balewski *et al.*, Phys. Lett. B **420**, 211–216 (1998).
11. S. Sewerin *et al.*, Phys. Rev. Lett. **83**, 682–685 (1999).
12. P. Kowina *et al.*, Eur. Phys. J. A **22**, 293–299 (2004).
13. R. Bilger *et al.*, Phys. Lett. **420**, 217–224 (1998).
14. S. Abd El-Samad *et al.*, Phys. Lett. B **632**, 27–34 (2006).
15. M. Fritsch, PhD thesis, University of Erlangen–Nürnberg (2002).
16. J. Przerwa, *these proceedings*.
17. W.–M. Yao *et al.*, J. Phys. G **33**, 1–1232 (2006).
18. F. Balestra *et al.*, Phys. Rev. C **63**, 024004–1–15 (2001).
19. M. Wolke, PhD thesis, University of Münster (1997).
20. C. Quentmeier *et al.*, Phys. Lett. B **515**, 276–282 (2001).
21. P. Winter *et al.*, Phys. Lett. B **635**, 23–29 (2006).
22. I. Keshelashvili, PhD thesis, University of Tbilisi (2006).
23. U. Tengblad, G. Fäldt, and C. Wilkin, Acta Physica Slovaca **56**, 205–211 (2006).
24. M. Hartmann *et al.*, Phys. Rev. Lett. **96**, 242301–1–4 (2006).
25. Y. Maeda *et al.*, (*in preparation*).
26. V. Kleber *et al.*, Phys. Rev. Lett. **91**, 172304–1–4 (2003); A. Dzyuba *et al.*, Eur. Phys. J. A **29**, 245–251 (2006); A. Dzyuba *et al.* (*in preparation*).
27. C. Wilkin, Phys. Rev. C **47**, R938–940 (1993).
28. J. Berger *et al.*, Phys. Rev. Lett. **61**, 919–922 (1988).
29. B. Mayer *et al.*, Phys. Rev. C **53**, 2068–2074 (1996).
30. J. Smyrski *et al.*, Phys. Lett. B **649**, 258–262 (2007).
31. T. Mersmann *et al.*, Phys. Rev. Lett. **98**, 242301–1–4 (2007).
32. P. Berthet *et al.*, Nucl. Phys. A **443**, 589–600 (1985).
33. C. Wilkin *et al.*, Phys. Lett. B (*in press*), arXiv:0707.1489.
34. J. Smyrski, *these proceedings*.